CMOS RF Mixer No-linearity Design

Qiang Li, Jinlong Zhang, Wei Li, and Jiann S. Yuan
Chip Design and Reliability Laboratory
School of Electrical Engineering and Computer Science
University of Central Florida, Orlando, Florida 32816

Abstract

Design Equations for the 1dB compression point and 3rd-order intermodulation point as a function of circuit and technology parameters are derived using Volterra series expansion. Linearity analysis for both single and double-balanced CMOS Gilbert Mixers is examined. The transconductance stage using inductive degeneration is more linear than that using capacitive or resistive degeneration, and the single-balanced mixer is more linear than the double-balanced one at the same bias current and transconductance. The analytical predictions are verified with the Cadence SpectreRF circuit simulation and experimental data. Good agreement between the model predictions and experimental data is obtained.

1. Introduction

CMOS RF up/down mixer results in a considerable increase in transceiver integration and a reduction in cost. The design of mixers faces many compromises between conversion gain, local oscillator (LO) power, linearity, noise figure, port-to-port isolation, voltage scaling, and power consumption [1]. Mixer linearity is a very important parameter in transceiver design, because system linearity is often limited by the first down-conversion mixer due to a relatively large signal compared with that at the LNA input. Since active FET mixers achieve conversion gain with lower LO power than their passive counterparts, the active CMOS single-balanced and double-balanced Gilbert mixers shown in Fig. 1 are commonly used in the CMOS transceiver design. Compared with the single-balanced counterpart, the double-balanced mixer has batter port-to-port isolation due to symmetrical architecture. The double-balanced mixer has higher noise figure due to more noise generators. The overall Gilbert mixer linearity is controlled primarily by the transconductance stage if the LO-driven transistors act as good switches. To improve the linearity, the transconductance stage is

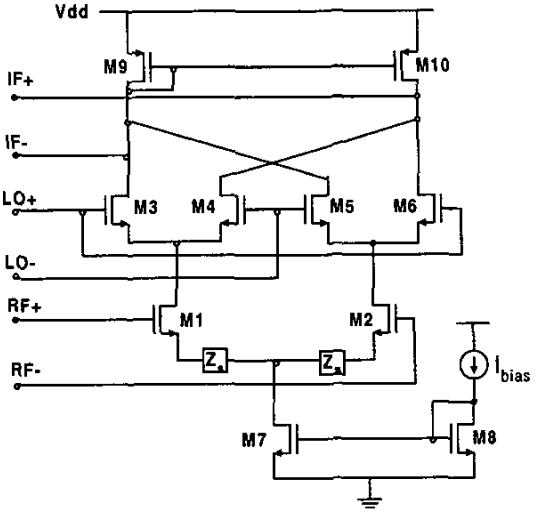

Fig. 1 Double-balanced CMOS mixer

usually degenerated by Z_S, which can be implemented by using either resistors, capacitors, or inductors. Good understanding of linearity from different degeneration architectures is desirable for mixer design. Mixer nonlinearity of bipolar circuits using Volterra series analysis was examined [2]. Short-channel MOSFET nonlinearity analysis using Taylor series expansion was also presented [3]. The assumption of ideal memoryless transfer nonlinearities in the Taylor series analysis, however, is unrealistic.

In this paper, RF nonlinearity equations using Volterra series technique [4,5] for both single and double-balanced CMOS Gilbert mixers including source degeneration are derived. Linearities of different degeneration techniques are examined. The analytical predictions are compared with the RF circuit simulation and experimental data.

2. IIP3 and 1dB compression point in Volterra series

 0-7803-7150-X/01/$10.00@2001 IEEE

For a weakly nonlinear circuit such as mixer and LNA having multiple non-commensurate small-signal excitations, the nonlinearities in these circuits are often so weak that they have a negligible effect on their linear response [4]. However the nonlinear phenomena (e.g., intermodulation distortion) in such quasilinear circuits can affect system performance significantly and thus are very important in the design of RF circuits.

For a general two-port system, one can write Volterra series expansion relating input and output variables as in (1). Let V and I be the input and output variables of the transconductance stage. Where v_{sig} is a small-input signal at DC bias V_{DC} and $A_n(\ ),\ n = 1, 2, \cdots$ are the Volterra series coefficients.

For a narrowband input signal $v_{sig} = Mcos(\omega_0 t)$, the corresponding narrowband output signal i_{sig} is determined by summing all $cos(\omega_0 t)$ terms yielding (2) The 1dB compression point can be computed by taking the ratio of all terms to its linear term $A_1(s)M$ in (2) and setting the ratio equal to -1dB (0.891) [3]. This results in

$$P_{1dB} = \frac{M_{odd}^2}{2R_S} \approx \left| \frac{A_1(s)}{13.8A_3(s_1,s_2,s_3)R_S} \right| \quad (3)$$

The input-referred third-order intercept point (P_{IIP3}) can be determined by substituting $v_{sig} = Mcos(\omega_1 t)+Mcos(\omega_2 t)$ into (1). The output signal components at frequency $2\omega_2 - \omega_1$ or $2\omega_1 - \omega_2$ determine the input-referred third-order intermodulation product, i.e.

$$|IM_3| = \left| \frac{3}{4} \frac{A_3(s_a,s_a,-s_b)}{A_1(2s_a - s_b)} M^2 \right| \cos((2\omega_1 - \omega_2)t) \quad (4)$$

Equating the amplitude of the intermodulation products term with that of linear term gives

$$P_{IIP3} = \frac{M_{3rd}^2}{2R_S} = \left| \frac{2A_1(s)}{3A_3(s_1,s_2,s_3)R_S} \right| \quad (5)$$

Note that IIP3 measures the small-signal nonlinearity dominated by the third-order nonlinearity and that P_{1dB} measures the large-signal nonlinearity from all odd-order terms.

3. Nonlinearity of active RF CMOS mixer

Figure 2 shows the small-signal model of the transconductance stage to derive the non-linearity equations for the single-balanced mixer. In this figure

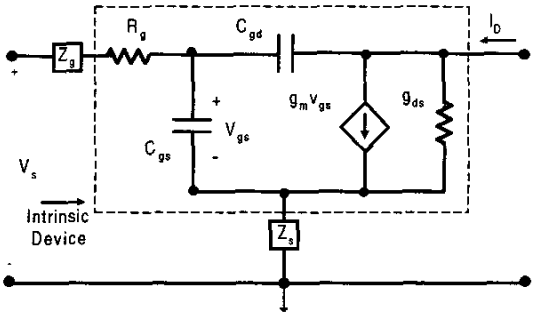

Fig. 2 Small-signal model of single-balanced mixer transconductance stage

V_s is the voltage signal source, Z_g is the impedance at the gate of M1 which includes source resistance R_s, gate resistance r_g, shunt impedance of bias circuit and impedance of impedance matching network, and Z_s is the impedance at the source of M1 which includes the parasitic source resistance r_s of M1 and the impedance of the degeneration elements (resistor, capacitor, and inductor). Aside from these external components, several elements such as gate-drain capacitance C_{gd}, gate-source capacitance C_{gs}, output conductance g_{ds}, and output transconductance g_m have been included in the MOSFET intrinsic device model. Using the model in Fig. 2, Kirchhoff's voltage law yields (5)
where

$$I_{ds} = \frac{g_{ds}(sC_{gd}V_{gs} + I_d - g_m V_{gs})}{g_{ds} + sC_{gs}}$$

$$I_{gd} = g_m Vgs - I_d + \frac{g_{ds}(sC_{gd}V_{gs} + I_d - g_m V_{gs})}{g_{ds} + sC_{gs}}$$

I_d is the drain signal current, V_{gs} is gate source signal voltage drop cross C_{gs}, and $s(= j\omega)$ is the Laplace variable. Using this relationship Volterra series expression of I_d is derived as (6)
where $A_1(s)$, $A_2(s_1,s_2)$ and $A_3(s_1,s_2,s_3)$ are the first three Volterra series coefficients given by (7)
T_1, T_2 and T_3 are the first three Taylor series coefficients of drain current and $C_1(s)$, $C_2(s)$ and $C_3(s)$ are the first three Volterra series coefficients of gate-source signal voltage.

From (7) the Volterra series coefficients are known. Substituting the result in (4) gives (8). The magnitude of $|IM_3|$ depends on

$$\left| 1 + j\omega C_{gs}[Z_s(\omega_1, L_s) + Z_g(\omega_1, L_s)] \right| \quad (9)$$

$$I(V_{DC} + v_{sig}) = A_1(s)v_{sig} + A_2(s_1,s_2)v_{sig}^2 + A_3(s_1,s_2,s_3)v_{sig}^3 + \ldots \quad (1)$$

$$i_{sig} = \left[A_1(s)M + \frac{3}{4}A_3(s_1,s_2,s_3)M^3 + \ldots + \frac{A_{2k-1}}{2^{2k-2}} \binom{2k-1}{k-1} M^{2k-1} \right] \cos(\omega_0 t) \quad (2)$$

$$V_s = (Z_g + R_g)(I_{gs} + I_{gd}) + V_{gs} + Z_s(I_{gs} + g_m V_{gs} + I_{ds}) \quad (5)$$

$$I_d = A_1(s)V_s + A_2(s_1,s_2)V_s^2 + A_3(s_1,s_2,s_3)V_s^3 + \ldots \quad (6)$$

$$A_1(s) = T_1C_1(s)$$

$$A_2(s_1,s_2) = T_1C_2(s_1,s_2) + T_2C_1(s_1)C_1(s_2) \quad (7)$$

$$A_3(s_1,s_2,s_3) = T_1C_3(s_1,s_2,s_3) + 2T_2\overline{C_1C_2} + T_3C_1(s_1)C_1(s_2)C_1(s_3)$$

$$|IM_3(\omega_1,\delta\omega,L_s)| = \left|\frac{3A_1^3(\omega_1)}{T_1^4}\right| |1 + j\omega C_{gs}[Z_s(\omega_1,L_s) + Z_g(\omega_1,L_s)]|T_3 - 2T_2\rho(\omega_1,\delta\omega,L_s)|M^2 \quad (8)$$

where $\rho(\omega_1,\delta\omega,L_s) = \frac{T_2}{T_1}[2A_1(\delta\omega,L_s)Z_s(\delta\omega,L_s) + A_1(2\omega_1,L_s)Z_s(2\omega_1,L_s)]$ and $\delta\omega = \omega_1 - \omega_2$

With inductive degeneration $j\omega C_{gs}Z_s(\omega_1,L_s)$ is a negative real number which cancels the "1" term partially. There is no such cancellation with resistive degeneration and capacitive degeneration, which indicates the same mechanism as in the bipolar case [2]. Expression (8) shows the third order intermodulation product dependence of source inductance of the single-balance CMOS mixer. More accurate, but less intuitive expressions for the input-referred 1dB compression point and third-order intercept point can be obtained by directly substitute Volterra series coefficient (7) into (3) and (5).

Similarly, the equivalent circuit shown in Fig. 3 is used to derive nonlinearity equations for the

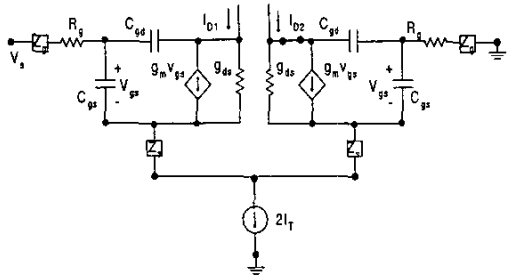

Fig. 3 Small-signal model of double-balanced mixer transconductance stage

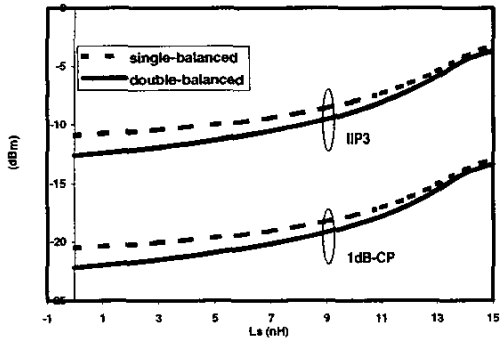

Fig.4. Mixer input-referred 1dB compression point and third-order intercept point as a function of source conductance

differential-pair transconductance stage of the double-balanced CMOS mixer. Double-balanced mixer input-referred third-order intercept point and 1dB compression point as a function of source inductance is shown in Fig. 4. The sinusoidal signals used are at 2.42 and 2.43 GHz, respectively and the LO frequency is at 2.45 GHz. Also shown in the figure are the single-balanced mixer input-referred third-order intercept point and 1dB compression point versus the source inductance. It is clear form Fig. 5 that the linearity of single balanced mixer is better than that of the double-balance one.

4. Results and discussions

A double-balanced mixer without using inductance degeneration was fabricated in TSMC 0.18 μm CMOS process, and its IIP3 was measured. Figure 5 displays the spectra seen at the IF output. The 3IM/IF ratio is -26.36 dBc at –25 dBm RF input power. IIP3 is –11.8 dB.

To validate the theory a double-balanced mixer in Fig. 1 is simulated using Cadence Spectre-RF. PSIN components at Cadence analog library are selected for both the RF input and IF output. The RF simulation reveals that the 3IM/IF ratio varies noticeably with respect to source inductance. Figure 6 compares the IF output spectra of mixer with and without source inductor. RF power is at -25 dBm. The 3IM/ IF ratio of mixer with 15 nH source inductor is -44 dBc. 3IM/ IF ratio of mixer without source inductor is -26 dBc. IIP3 is increased by 9 dB with the source inductance degeneration. Figure 7 shows IIP3 as a function of source inductance predicted by the analytical equations and RF circuit simulation. Good agreement between the simulation results and analytical predictions is obtained. Experimental data of IIP3 without source inductance degeneration ($L_s = 0$) is also given in this plot. It is clear from Fig. 8 that the larger the source inductance degeneration, the higher IIP3. However, the mixer voltage gain decreases as the source inductance increases. That's because Q of the input circuit is reduced with increasing source inductance

degeneration. The gain is decreased by 5 dB when a 15 nH inductor is used. Figure 8 shows the overall voltage gain and single sideband noise figure before and after design improvement. The low frequency noise figure is due to 1/f noise. Noise figure reaches the minimum around 100 MHz. The increase of noise figure after 100 MHz is due to a decrease in conversion gain. The peak is around 2.5 GHz while 1/f noise mixes up to the LO frequency.

5. Summary

Closed-form analytical equations for the CMOS RF mixer linearity using Volterra series expansion are derived. The Volterra series technique is more realistic because it does not require an assumption of memoryless transfer nonlinearities. The design methodology to achieve high linearity for given noise figure and conversion gain is presented. The design of the mixer has been verified by using the Cadence SpectreRF simulation and experimental data. Good agreement between the analytical predictions and the Cadence RF simulation has been obtained. The mixer linearity can be improved by tuning gm stage source inductance and the gate overdrive voltage.

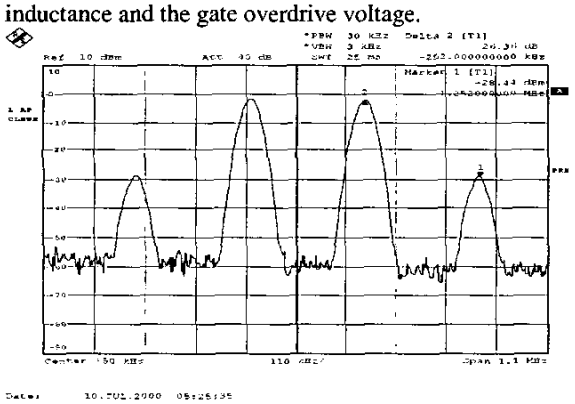

Fig.5. Measured IF output spectra (RFin -35dBm)

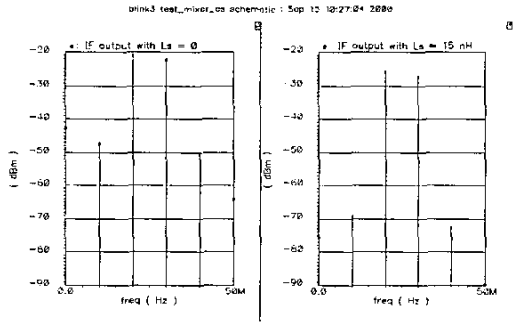

Fig. 6. Simulated mixer IF output spectra with and without source inductance degeneration

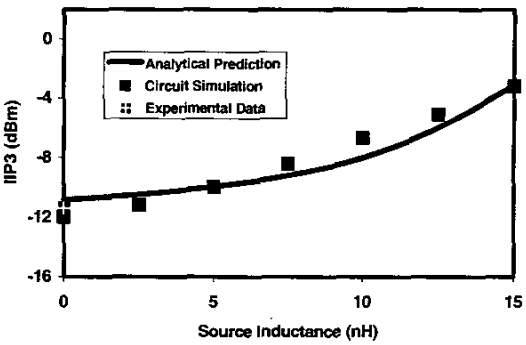

Fig.7 Analytical prediction and simulation result as a function of source inductance

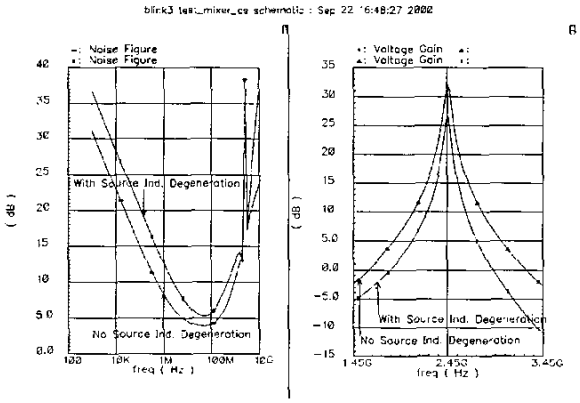

Fig.8 Mixer voltage gain and noise figure versus frequency

References

[1] P. J. Sullivan, B. A. Xavier, and W. H. Ku, "Low voltage performance of a microwave CMOS Gilbert cell," *IEEE J. Solid-State Circuits,* vol. JSSC-33, pp. 1151-1155, July 1997

[2] K. L. Fong and R. G. Meyer, "High-frequency nonlinearity analysis of common-emitter and differential-pair transconductance stages," *IEEE J. Solid-State Circuits,* vol. JSSC-33, pp. 548-555, April 1998

[3] T. Soorapanth and T. H. Lee, "RF linearity of short-channel MOSFETs," *First International Workshop on Design of Mixed-Mode Integrated Circuits and Applications*, Cancun, Mexico, July 28-30, 1997, pp. 81-84

[4] D. D. Weiner and J. F. Spina, *Sinusoidal Analysis and Modeling of Weakly Nonlinear Circuits.* van Nostrand Reinhold: New York, 1980

[5] S. A. Mass, *Microwave Mixer.* Artech House: Norwood, MA, 1993

[6] Q. Huang, P. Orsatti, and F. Piazza, "GSM Transceiver Front-End Circuits in 0.25-μm CMOS", *IEEE J. Solid-State Circuits,* vol. JSSC-34, pp. 292-303, March 1999